

This article was downloaded by:

On: 25 January 2011

Access details: *Access Details: Free Access*

Publisher *Taylor & Francis*

Informa Ltd Registered in England and Wales Registered Number: 1072954 Registered office: Mortimer House, 37-41 Mortimer Street, London W1T 3JH, UK



## Liquid Crystals

Publication details, including instructions for authors and subscription information:

<http://www.informaworld.com/smpp/title~content=t713926090>

### Observations of focal conic domains in smectic liquid crystals aligned on patterned self-assembled monolayers

J. P. Bramble<sup>a</sup>; S. D. Evans<sup>a</sup>; J. R. Henderson<sup>a</sup>; T. J. Atherton<sup>b</sup>; N. J. Smith<sup>c</sup>

<sup>a</sup> Molecular and Nanoscale Physics Group, School of Physics and Astronomy, University of Leeds, Leeds, UK <sup>b</sup> Thin Film and Photonics Group, School of Physics, Exeter, UK <sup>c</sup> Sharp Laboratories of Europe Ltd, Oxford, UK

**To cite this Article** Bramble, J. P. , Evans, S. D. , Henderson, J. R. , Atherton, T. J. and Smith, N. J.(2007) 'Observations of focal conic domains in smectic liquid crystals aligned on patterned self-assembled monolayers', *Liquid Crystals*, 34: 10, 1137 – 1143

**To link to this Article:** DOI: 10.1080/02678290701618351

**URL:** <http://dx.doi.org/10.1080/02678290701618351>

PLEASE SCROLL DOWN FOR ARTICLE

Full terms and conditions of use: <http://www.informaworld.com/terms-and-conditions-of-access.pdf>

This article may be used for research, teaching and private study purposes. Any substantial or systematic reproduction, re-distribution, re-selling, loan or sub-licensing, systematic supply or distribution in any form to anyone is expressly forbidden.

The publisher does not give any warranty express or implied or make any representation that the contents will be complete or accurate or up to date. The accuracy of any instructions, formulae and drug doses should be independently verified with primary sources. The publisher shall not be liable for any loss, actions, claims, proceedings, demand or costs or damages whatsoever or howsoever caused arising directly or indirectly in connection with or arising out of the use of this material.

# Observations of focal conic domains in smectic liquid crystals aligned on patterned self-assembled monolayers

J.P. BRAMBLE†, S.D. EVANS\*†, J.R. HENDERSON†, T.J. ATHERTON‡ and N.J. SMITH§

†Molecular and Nanoscale Physics Group, School of Physics and Astronomy, University of Leeds, Woodhouse Lane, Leeds, LS2 9JT, UK

‡Thin Film and Photonics Group, School of Physics, Stocker Road, Exeter, EX4 4QL, UK

§Sharp Laboratories of Europe Ltd, Edmund Halley Road, Oxford Science Park, Oxford, OX4 4GB, UK

(Received 18 June 2007; accepted 8 August 2007)

Patterned Self-Assembled Monolayers (SAMs) promoting both homeotropic and planar degenerate alignment of *n*CBs in their smectic-A phase were created using microcontact printing of functionalized organothiols on gold films. By patterning the surface with homeotropic and planar aligning SAMs, the location and formation of the focal conic domains (FCDs) can be controlled. Polarizing microscopy was used to study the formation of FCDs in circle, stripe and checkerboard pattern geometries. Fluorescent confocal microscopy (FCM) was used for the first time to measure the eccentricity of FCDs that form along a stripe pattern.

## 1. Introduction

In the smectic-A phase, liquid crystal (LC) molecules form into fluid layers, with the LC director perpendicular to the layer normal. When aligned between two surfaces that promote homeotropic alignment, the layers form parallel to the surfaces, but when confined to a thin cell consisting of a planar aligning surface and a homeotropic aligning surface, smectic-A phase LCs form into focal conic domains (FCDs) [1, 2]. The FCD structures form to minimize the energy cost of deforming smectic layers to match the antagonistic boundary conditions. In a FCD the molecular layers are described by surfaces which are perpendicular to a straight line joining a point on an ellipse and a point on a hyperbola. The ellipse and hyperbola are cofocal and are described by the following equations [1]:

$$\frac{x^2}{a^2} + \frac{y^2}{b^2} = 1, \quad z=0 \quad (1)$$

$$\frac{x^2}{a^2-b^2} - \frac{z^2}{b^2} = 1, \quad y=0 \quad (2)$$

where the eccentricity of the ellipse is defined by

$$e = \frac{\sqrt{a^2-b^2}}{a}. \quad (3)$$

It is possible from this description to distinguish three types of FCDs [1]. We limit our description to FCDs of negative gaussian curvature, otherwise known as focal conic domains of the first species (FCD-I). These surfaces are also known as Dupin cyclides. When a FCD has zero eccentricity, it is known as a toroidal focal conic domain (TFCD), the ellipse becomes a circle and the hyperbola a straight line. Figure 1 shows the layer structure found in a FCD of zero and non-zero eccentricity. A complete domain is bounded by two semi-infinite cylinders with the ellipse as a common centre. Figure 1 shows the upper half of a complete domain. Friedel's laws of association are empirical laws derived from observations of smectic films. In fact, Friedel determined the layered structure of smectic phases by studying the geometrical defects that could be seen [4]. The laws ensure that the layer spacing is constant and that space is filled with continuous layers. The first is the law of impenetrability which states that two FCDs cannot penetrate each other and if they are in contact at any point they are in tangential contact. Recent studies of smectic LCs confined in etched channels have shown that regular arrays of TFCDs can be formed [5]. These systems have been studied using atomic force microscopy [6].

Self-assembled monolayers (SAMs) of functionalized organothiols on gold can be used to align LCs in the nematic and smectic phases. In this study, regions of homeotropic and planar aligning SAMs were microcontact printed onto thin gold films to create

\*Corresponding author. Email: s.d.evans@leeds.ac.uk

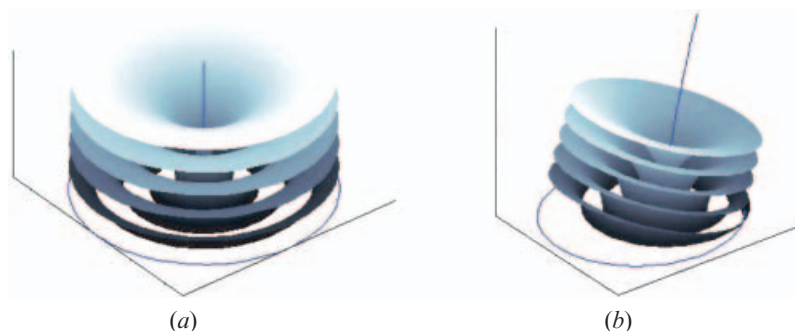


Figure 1. FCDs of the first species (FCD-I) with (a) zero eccentricity, (b) eccentricity  $e=0.3$ . The surfaces shown represent smectic layers within the FCD. The top surface shown is curved, and this becomes flat as additional layers are added to the diagram. Recreated with MATLAB using parametric equations and values taken from [3].

micropatterned surfaces. Microcontact printing of SAMs enabled us to create regions of different alignment on a similar scale to that of the FCDs. By controlling the size and geometry of the chemical surface pattern, we can control the formation and nature of the FCDs that form in the smectic-A phase.

## 2. Experimental

Patterned surfaces were prepared using microcontact printing of functionalized organothiols on thin gold films. Glass slides were cleaned rigorously with detergent, MilliQ water (Millipore), methanol, piranha etch (30% hydrogen peroxide, 70% sulphuric acid) and finally MilliQ water. The substrates were dried in nitrogen and mounted in a thermal evaporator (Edwards Auto 306). A 3 nm adhesion layer of Cr was deposited, followed by the deposition of a 25 nm Au film. This thickness is sufficient to create a continuous gold film yet remain optically transparent, and hence it is suitable for polarizing microscopy studies. The substrates were rotated during evaporation to ensure there was no anisotropy in the formation of gold grains, which can lead to increased azimuthal anchoring [7]. Polydimethylsiloxane (PDMS) (Dow Corning Corporation) was prepared for microcontact printing as described by Kumar and Whitesides [8]. The PDMS was well mixed and degassed under vacuum. A silicon wafer, etched with a series of micrometre-sized features was used as a master for the formation of PDMS stamps. The wafer was silanized, to aid stamp removal, by immersion in a 1% solution of perfluoro-decyltriethoxysilane (Fluorochem Ltd) in DCM for 1 hour. For circular structures, masters were made using negative tone photoresist SU8 2010 (Micro Chem Corporation) on glass substrates. These masters were silanized with the same silane via the vapour phase. The

PDMS material was poured onto the master in a mould and cured at 60°C for 10 hours. After curing, the PDMS was removed and cut into small stamps. The  $\text{CF}_3$ -terminated SAMs promote homeotropic alignment of the LC  $n\text{CB}$  where  $6 \leq n \leq 9$ , and the  $\text{COOH}$ -terminated SAMs promote planar degenerate alignment of the LC  $n\text{CB}$  where  $5 \leq n \leq 9$  in the nematic phase [9, 10], and also for 8CB and 9CB in the smectic-A phase [11]. A 7 mM ethanolic solution of  $\text{HS}-(\text{CH}_2)_{17}-(\text{CF}_2)_9-\text{CF}_3$  was prepared. The printing surface of the stamp was inked with this solution for a few minutes and then carefully dried with nitrogen. The stamp was then placed onto the gold surface for 2 minutes. The gold surfaces were then immersed in a 3 mM ethanolic solution of 11-mercaptoundecanoic acid,  $\text{HS}-(\text{CH}_2)_{10}-\text{COOH}$  (Sigma-Aldrich), for 12 hours. This back fills the non-printed regions to produce a two-component patterned surface. LC cells were formed with a homeotropic aligning top surface. Cell gaps were maintained with two 23  $\mu\text{m}$  thick stripes of polyethylene terephthalate (PET). The samples were heated above the nematic-isotropic transition temperature of the LC to be investigated and a small amount of LC (Kingston Chemicals, UK) was placed on the patterned surface before the upper surface was placed on top. The samples were then slowly cooled ( $0.1^\circ\text{C min}^{-1}$ ) into the smectic phase. For dual patterned surface studies, the features were aligned carefully in the smectic phase, heated into the isotropic phase and slowly cooled back into the smectic phase. The rate of cooling is important to ensure that the minimum number of FCDs form in the patterned regions.

Typically, we used 9CB, which has a smectic-A phase between 42°C and 48°C, to explore the formation of FCDs. In order to investigate the three-dimensional structure of the FCD using fluorescent confocal microscopy (FCM), 8CB, which has a smectic-A phase

at room temperature, was used. 8CB was mixed with fluorescent dye BTBP (Sigma Aldrich, CAS 83054-80-2) at a concentration of 0.1%wt. BTBP is an anisotropic molecule which is known to align with the LC. It has been used in previous FCM studies of LCs to determine the three-dimensional orientational order in smectic defects [12].

### 3. Results

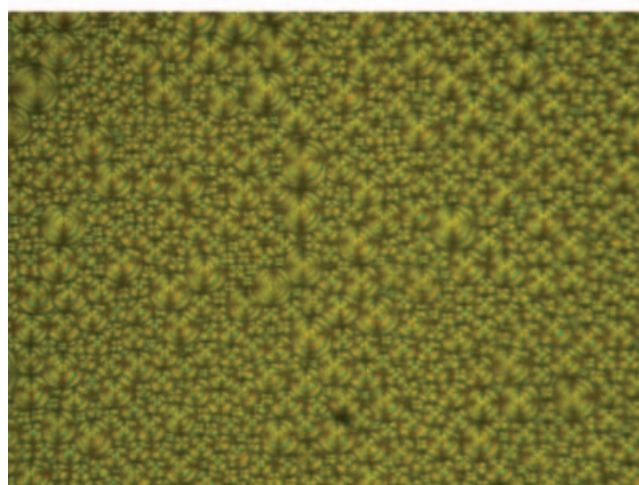
Figure 2(a) shows the formation of random FCDs in a LC cell with a non-patterned planar aligning COOH-terminated SAM lower surface and a homeotropic aligning CF<sub>3</sub>-terminated SAM top surface. Figure 2(b) shows a polarizing microscopy image of 9CB aligned on circular planar regions. No transmission was seen in the homeotropic aligning regions indicating that the smectic layers are parallel to the surface in these regions. The circular regions contain either single or multiple FCDs. When the circular domains are larger than 20 μm, multiple FCDs form more frequently, and below 20 μm, increasingly only one FCD forms in each region. The entire printed region is about 1 cm<sup>2</sup> and it is filled with a vast number of domains spaced on a regular grid.

From the observations of the FCDs we can see that the base of the FCD does not protrude outside the

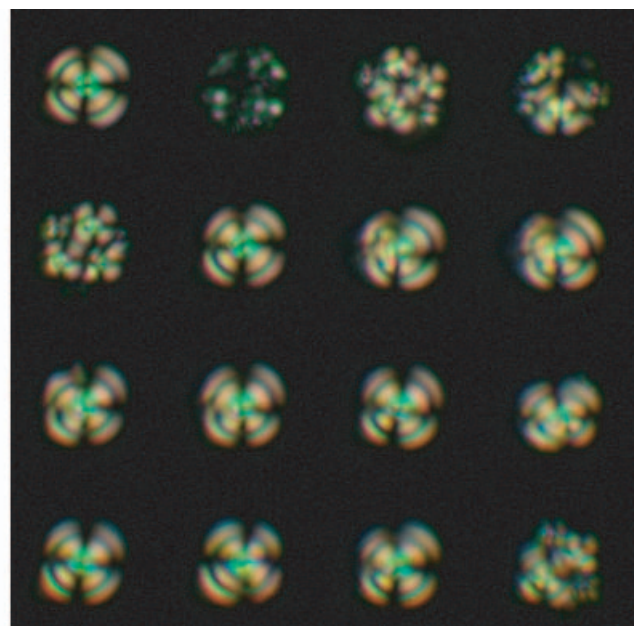
patterned region and that the FCDs fill the circles according to Friedel's laws of association. The chemical patterning therefore acts as a boundary which controls the position of FCDs on a surface.

Figure 3(a) shows the formation of FCDs on stripes of a planar aligning SAM, surrounded by a homeotropic aligning SAM. As for the circular patterns, FCDs form in the planar regions. The width of the stripes confines the size of the FCD. When the stripe width is 10 μm or less, one FCD forms across the stripe width. As the FCDs are identical in size, they form regularly down the stripes. FCDs continue to be formed on stripes with widths of 2 μm, but become increasingly difficult to image at smaller scales.

Using polarizing microscopy alone it appears that the FCDs are circular in the plane of the surface; this would mean that the eccentricity of the FCD is zero and hence the defects are toroidal. For a FCD with semiminor axis of 5 μm and eccentricity of 0.3, the semimajor axis would be just 5.24 μm, which would be difficult to measure accurately using polarizing microscopy. The hyperbolic disclination in the centre of a FCD changes more significantly for small values of eccentricity. FCM was used to obtain three-dimensional images of the FCDs. Figure 4 shows a slice through the centre of a number of FCDs aligned on a 10 μm stripe. Increased brightness in the core of the defect is due to the higher concentration of



(a)



(b)

Figure 2. Polarizing microscopy images of 9CB in a cell with (a) a planar aligning COOH-terminated SAM lower surface and a homeotropic aligning CF<sub>3</sub>-terminated SAM top surface, where FCDs form with random sizes and positions (image width 500 μm), and (b) lower surface patterned with 20 μm diameter circles of planar aligning COOH-terminated SAM surrounded by CF<sub>3</sub>-terminated SAM. Crossed polarizers are set parallel to the image edges.

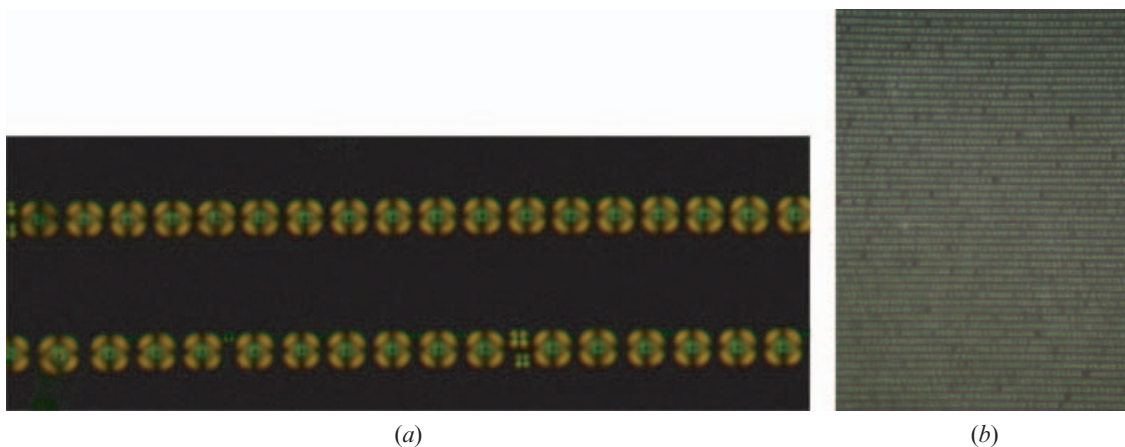


Figure 3. Polarizing microscopy images of 9CB aligned on stripes of COOH-terminated SAM surrounded by CF<sub>3</sub>-terminated SAM. Crossed polarizers are set parallel to the image edges. (a) 10 μm planar stripe with 30 μm periodicity; (b) 2 μm planar stripe with 4 μm periodicity.

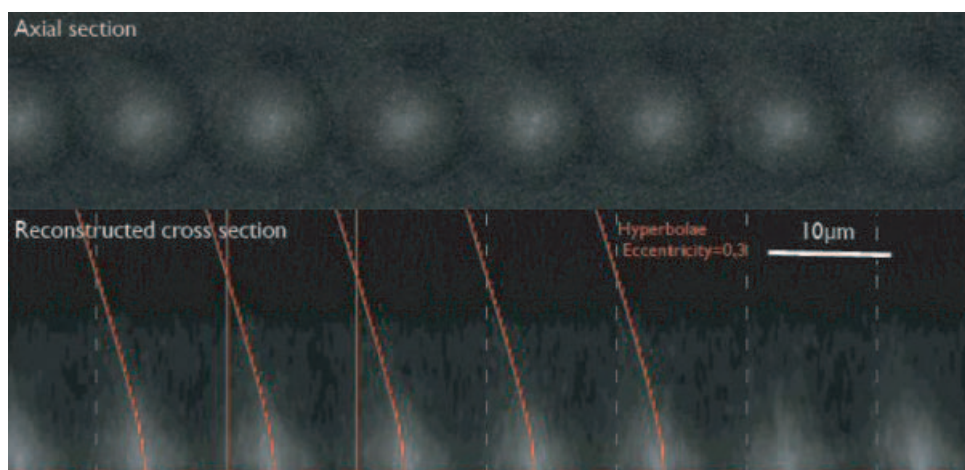


Figure 4. Fluorescent confocal polarizing microscopy images of FCDs aligned on a 10 μm planar stripe. The top image is a plan view of the FCDs and the lower view is a cross section, reconstructed from multiple images taken at different depths of focus.

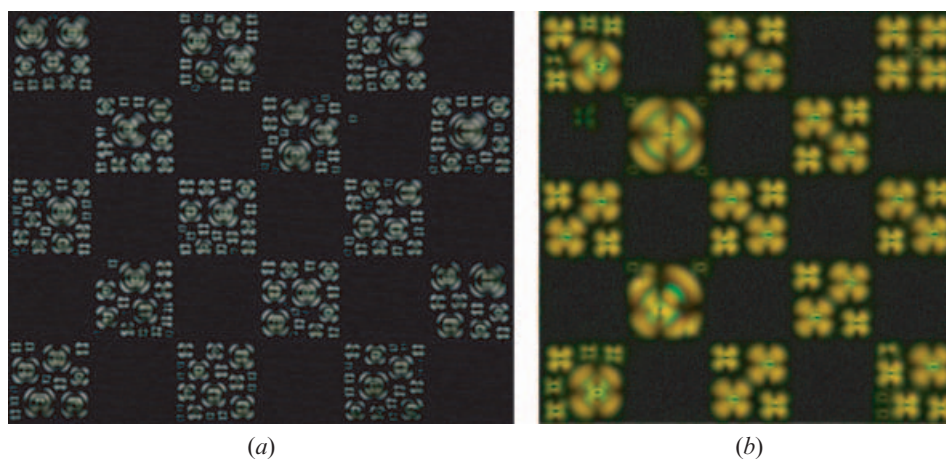


Figure 5. Polarizing microscopy images of 9CB aligned on a checkerboard pattern with a square size of length (a) 16 μm and (b) 8 μm. Crossed polarizers are set parallel to the image edges.

dye in the core. This image clearly shows that the core is in fact hyperbolic in shape, and therefore the FCDs have non-zero eccentricity and are elliptical with the semimajor axis along the direction of the stripes.

A hyperbolic function can be fitted to the image to extract a value for the eccentricity of the FCD. We find a value of  $e=0.3\pm 0.05$ . This must satisfy a minimum energy condition for the system as a whole. Theory derived by Kleman and Lavrentovich [1] implies that the stripe width and eccentricity can be used to calculate the value of the energy of a FCD. This theory, however, assumes that the domain is isolated, which is clearly not the case in this system. The effect of the boundary and the interaction between neighbouring domains must be taken into consideration. This technique for confining the boundaries could lead to a method of finding the energy of FCDs of different sizes and eccentricities. It is found that, at tilt grain boundaries in smectic-A LCs, FCDs are formed with ellipses of equal eccentricities and parallel long axes [13, 2], and this is exactly what is seen on a striped surface, where the surface acts as the boundary. For an excellent illustration of this structure and further discussion see [13].

Checkerboard patterns confine the formation of the FCDs to squares. As with the stripe geometry, the number of FCDs that can form is governed by the size of the planar aligning region. Figure 5(a) shows that on average 12 FCDs form above the  $16\mu\text{m}$  square planar region. These arrangements show a number of different sized FCDs, they do not appear to be arranged in a regular fashion. However, as the size of the planar region is reduced, the number of FCDs

is reduced. Additionally, these domains show a regularity in their formation above the planar region. Figure 5(b) shows the regular arrangement of FCDs above an  $8\mu\text{m}$  square planar region. Again, we see discrete domain sizes. In the case of equal-sized FCDs, the formation is symmetrical. Figure 6 shows the distribution of FCD sizes for  $8\mu\text{m}$  and  $16\mu\text{m}$  checkerboard patterns.

Two patterned surfaces were used to make a cell with stripes on both sides. The stripes were aligned out of phase with each other so that when regions have antagonistic boundary conditions FCDs form on both surfaces. By changing the focus point we can see that the larger circular base is at the planar aligning surface. This is seen in Figure 7. When the patterned areas just overlap, FCDs no longer form and alignment in these regions is a smectic texture where the layers are aligned vertically to join the planar regions at each boundary.

#### 4. Discussion

The experimental results display two regimes. The first regime is when the natural size of the FCD is smaller than the pattern size. The FCDs either, for very large patterns, fill the space in a random matrix, or for smaller patterns begin to fill the space in a symmetrical arrangement, as in the smaller checkerboard geometry. The limiting case of this regime is where either one FCD forms, as in the circle geometry, or where the FCDs assemble into one-dimensional arrays along stripes. The second regime is when the pattern dimension is smaller than the natural size of the FCD and the FCD becomes

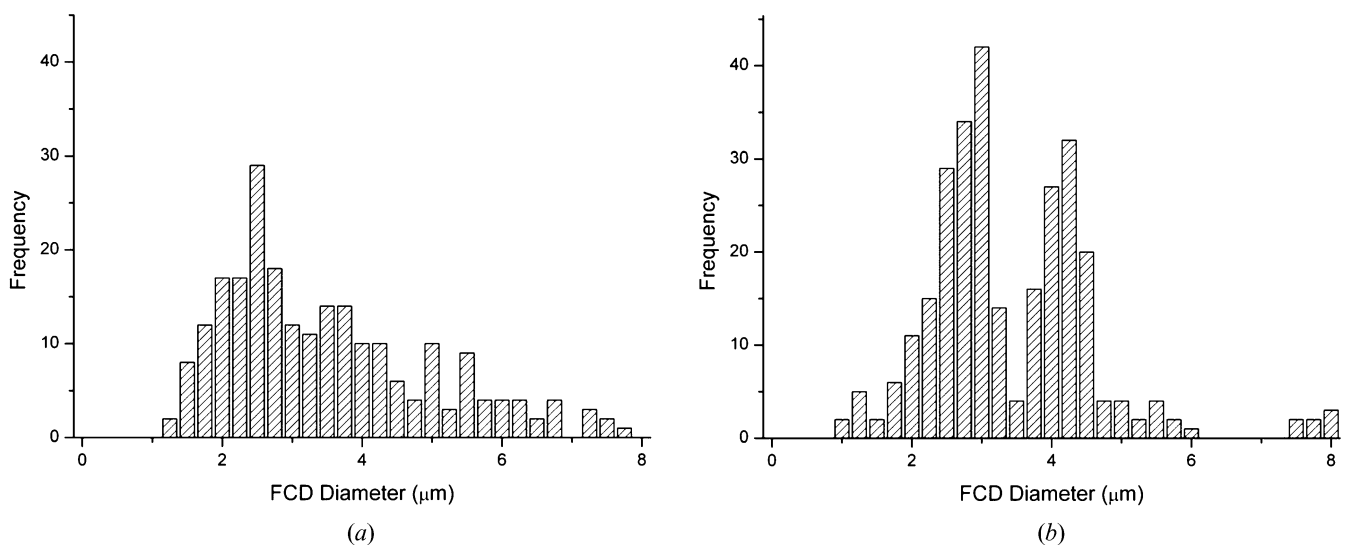


Figure 6. The distribution of FCD sizes when confined to (a)  $16\mu\text{m}$  checkerboards and (b)  $8\mu\text{m}$  checkerboards.

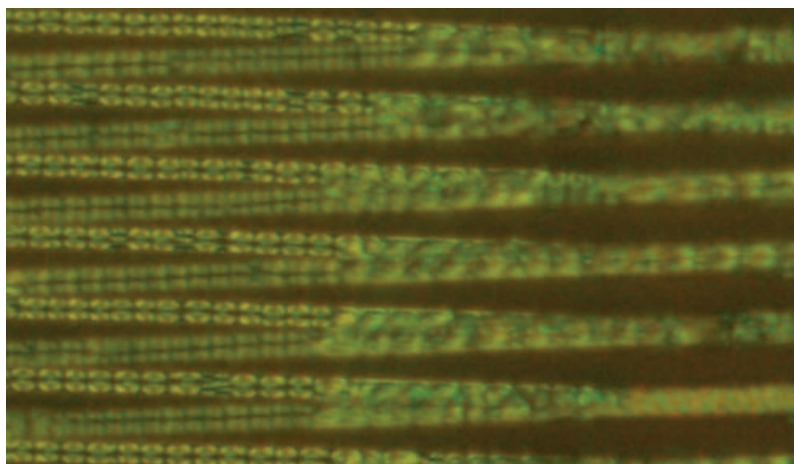


Figure 7. Polarizing microscopy image of 9CB aligned between two surfaces each patterned with  $10\ \mu\text{m}$  planar stripes and  $30\ \mu\text{m}$  periodicity. The stripes have been offset to observe the influence of the opposing surface on the nature of the smectic defects.

confined. For circle and checkerboard geometries, the FCD is confined on all sides and must become smaller. For the stripe geometry the situation is more interesting because the FCDs are only fixed in size in one dimension, across the stripe width, but are free along the stripes. FCM has shown that the FCDs adopt a configuration with non-zero eccentricities and parallel axes. The configuration must minimize the energy of not just the FCDs but of the entire system. Elastic theory [1, 2] predicts that the total curvature energy of the FCD is dependent on the size of the domain, the eccentricity and the material parameters, including the splay-bend and splay constants. For a FCD with non-zero eccentricity the smectic layers are tilted with respect to the layers outside the FCD (the homeotropic aligning stripes in our case). To resolve the mismatch there should be a set of dislocations outside the FCDs which prefer the eccentricity to tend to zero; without this contribution elastic theory would predict an unphysical eccentricity of unity [1, 2]. Our data for the stripe geometry implies that the defects adopt a compromise value of the eccentricity. The self-assembly (spacing) of the FCDs along the stripes may also be affected by these considerations. The experimental system described here can provide a controllable system where such considerations can be studied, for example, as a function of stripe width. Further experiments are planned to include FCM measurements of the FCD eccentricity as a function of the planar aligning stripe width and also to investigate any possible registry of FCDs due to the matching of dislocations in the homeotropic region between neighbouring stripes by varying the homeotropic aligning stripe width.

In conclusion, patterned self-assembled monolayers of functionalized organothiols on gold have been used to control the formation of focal conic domains in smectic-A LCs. Circular planar regions of  $10\ \mu\text{m}$  diameter allow one FCD to form. Stripe geometries of  $10\ \mu\text{m}$  width also allow one FCD to form regular one-dimensional arrays of FCDs. FCM reveals that the core of the FCD has non-zero eccentricity in stripe geometry. We find that the eccentricity has a value of around  $0.3 \pm 0.05$  for a stripe width of  $10\ \mu\text{m}$ .

#### Acknowledgments

This work was supported by the Engineering and Physical Research Council, grant No. GR/S59826/01. JPB and TJA acknowledge Sharp Laboratories of Europe, Ltd for the provision of CASE awards.

#### References

- [1] M. Kleman, O.D. Lavrentovich. *Phys. Rev. E*, **61**, 1574–1578 (2000).
- [2] M. Kleman, O.D. Lavrentovich. *Soft Matter Physics*. Springer (2003).
- [3] I.W. Stewart. *The Static and Dynamic Continuum Theory of Liquid Crystals*. Taylor and Francis (2004).
- [4] G. Friedel, F. Grandjean. *Bull. Soc. Franc. Miner.*, **33**, 409 (1910).
- [5] M.C. Choi, T. Pfohl, Z. Wen, Y. Li, M.W. Kim, J.N. Israelachvili, C.R. Safinya. *Proc. Natl. Acad. Sci. Unit. States. Am.*, **101**, 17340–17344 (2004).
- [6] V. Designolle, S. Herminghaus, T. Pfohl, Ch. Bahr. *Langmuir*, **22**, 363–368 (2006).
- [7] V.K. Gupta, N.L. Abbott. *Langmuir*, **12**, 2587–2593 (1996).
- [8] A. Kumar, G.M. Whitesides. *Appl. Phys. Lett.*, **63**, 2002–2004 (1993).

- [9] B. Alkhairalla, H. Allinson, N. Boden, S.D. Evans, J.R. Henderson. *Phys. Rev. E*, **59**, 3033 (1999).
- [10] B. Alkhairalla, N. Boden, E. Cheadle, S.D. Evans, J.R. Henderson, H. Fukushima, S. Miyashita, H. Schonherr, G.J. Vancso, R. Colorado Jr, M. Graupe, O.E. Shmakova, T.R. Lee. *Europhys. Lett.*, **59**, 410–416 (2002).
- [11] Y.L. Cheng, D.N. Batchelder, S.D. Evans, J.R. Henderson, J.E. Lydon, S.D. Ogier. *Liq. Cryst.*, **27**, 1267–1275 (2000).
- [12] I.I. Smalyukh, S.V. Shiyanovskii, O.D. Lavrentovitch. *Chem. Phys. Lett.*, **336**, 88–96 (2001).
- [13] M. Kleman, O.D. Lavrentovitch. *Eur. Phys. J. E*, **2**, 47–57 (2000).